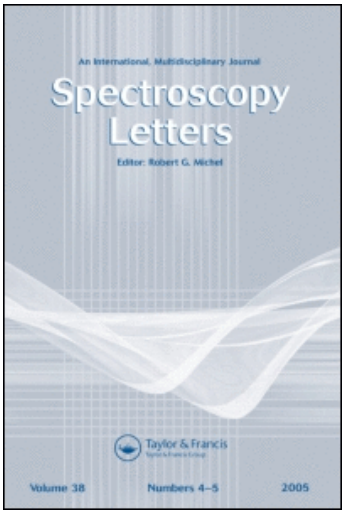

Spectroscopy Letters
Publication details, including instructions for authors and subscription information:
http://www.informaworld.com/smpp/title~content=t713597299

Experimental and Theoretical Study of the Electrochemical Behavior of *o*-Benzoquinone and Pyrocatechol

Yuan-zhi Song[a]
[a] Jiangsu Province Key Laboratory for Chemistry of Low-Dimensional Materials, Chemistry Department, Huaiyin Teachers College, Huaian, People's Republic of China

To cite this Article Song, Yuan-zhi(2007) 'Experimental and Theoretical Study of the Electrochemical Behavior of *o*-Benzoquinone and Pyrocatechol', Spectroscopy Letters, 40: 6, 811 — 833
To link to this Article: DOI: 10.1080/00387010701429682
URL: http://dx.doi.org/10.1080/00387010701429682

Spectroscopy Letters, 40: 811–833, 2007

ISSN 0038-7010 print/1532-2289 online
DOI: 10.1080/00387010701429682

Experimental and Theoretical Study of the Electrochemical Behavior of *o*-Benzoquinone and Pyrocatechol

Yuan-zhi Song
Jiangsu Province Key Laboratory for Chemistry of Low-Dimensional Materials, Chemistry Department, Huaiyin Teachers College, Huaian, People's Republic of China

Abstract: The geometric parameters, vibrational frequencies, and the thermochemical values of *o*-benzoquinone (*o*-BQ), *p*-benzoquinone (*p*-BQ), pyrocatechol (PC), and *p*-hydroquinone (*p*-HQ) were computed using *ab initio* calculation (HF) and density functional theory (DFT) with the 6-31G (d) and 6-31G (d, p) basis sets, respectively. Cyclic voltammetry with a gold electrode of PC solutions in phosphate buffers at pH 7.30 showed that the standard electrode potential of half reaction for *o*-BQ and PC is 0.813 V. The standard electrode potential of half reaction for *o*-BQ and PC with a *p*-BQ, H^+/*p*-hydroquinone (*p*-HQ) reference electrode, using the solvation energies and the sum of electronic and thermal free energies of *o*-BQ and PC, is consistent with the experimental one.

Keywords: *o*-Benzoquinone (*o*-BQ), cyclic voltammetry, DFT, HF, pyrocatechol (PC), standard electrode potential

INTRODUCTION

Pyrocatechol as a basic structure of adrenoceptor agonists, often called catechol, is an electron carrier. Numerous observations on the electrochemical behavior of catechols and their analogues such as epinephrine have been made

Received 4 September 2006, Accepted 10 April 2007
Address correspondence to Yuan-zhi Song, Jiangsu Province Key Laboratory for Chemistry of Low-Dimensional Materials, Chemistry Department, Huaiyin Teachers College, Huaian 223300, People's Republic of China. E-mail: songyuanzhi@126.com or songyuanzhi@sina.com

by many research groups.[1–10] The standard electrode potential, an important parameter, is a descriptor of molecular activity in biochemistry, pharmacy, analytical chemistry, and so forth. Hence it is important to investigate its chemistry property based on theoretical study.[11–13]

It is easy to calculate the transformed Gibbs free energies ($\Delta_r G^o$) of a redox reaction using quantum chemistry, for example, a redox reaction can be divided into the following two half reactions, which are written as

$$o\text{-Benzoquinone } (o\text{-BQ}) + 2H^+ + 2e^- = \text{pyrocatechol (PC)} \quad (1)$$

$$p\text{-Benzoquinone } (p\text{-BQ}) + 2H^+ + 2e^- = p\text{-hydroquinone } (p\text{-HQ}) \quad (2)$$

Thus, the reaction in water can be written as

$$o\text{-BQ}_{(l)} + p\text{-HQ}_{(l)} = \text{PC}_{(l)} + (p\text{-BQ})_{(l)}. \quad (3)$$

$\Delta_r G^o$ is calculated using the thermochemical values of *o*-BQ, PC, *p*-BQ, and *p*-HQ from Gaussian03 software. The standard electrode potential (E^o) of reaction (1) is calculated as

$$\Delta_r G^o = -nF(E^o - E^o_{p\text{-BQ/HQ}}) = -nF(E^o - E^o_{p\text{-BQ}/p\text{-HQ}}),$$

where n is the number of electrons involved, F is the Faraday constant $= 96.485^\circ\text{C mol}^{-1}$, and $E^o_{p\text{-BQ}/p\text{-HQ}}$ represents the standard electrode potential of half reaction for p-BQ/p-HQ.

In this paper, the geometries for *o*-BQ, *p*-BQ, *p*-HQ, and PC were calculated using *ab initio* calculation (HF) and density functional theory (DFT); furthermore, the standard electrode potential of half reaction for *o*-BQ and PC was also calculated at the same level and compared with the experimental result.

MATERIALS AND METHODS

PC used in this study was a commercial product (parity $>99.99\%$) purchased from Sigma. Phosphate buffers were prepared by titration of analytical reagent grade phosphoric acid with sodium hydroxide until the required pH value is achieved. A CHI660B Electrochemical Analyzer (CH Instrument, Austin, TX, USA) equipped with a computer as control and recorder was used. Conventional voltammetric experiments in phosphate buffers were performed at a scan rate of $0.1\ \text{Vs}^{-1}$ (step width 1 mV) with a 1-mm gold disk working electrode and a saturated calomel reference electrode (SCE). A platinum wire served as the auxiliary electrode. The working electrode was polished with 5 μm then 1 μm alumina slurries and ultrasonicated in turn with acetone and water for 3 min, respectively. Before each test, nitrogen was passed through the buffer solution for 15 min to drive off oxygen.

Calculations

The calculations were performed with the Gaussian03 program package.[14] The molecule was fully optimized using the RHF[15,16] and RB3LYP[17,18] methods with the 6-31G (d)[19] and 6-31G (d, p)[20] basis sets, respectively. The thermochemical values of *o*-BQ, *p*-BQ, *p*-HQ, and PC in gas state at 1 atm, 298.15 K, were also calculated at the same level. The solvation energies of *p*-BQ, *p*-HQ, PC, and *o*-BQ in water at 298.15 K, 1 atm, were calculated by the polarized continuum (overlapping spheres) model (PCM) of Tomasi and co-workers.[21–23]

RESULTS

Geometry

The optimized geometry is the most important step for calculation of the standard electrode potential of half reaction for *o*-BQ and PC because the thermochemical values of *o*-BQ and PC are controlled by the molecular geometries.

Two conformers of PC are computed. The optimized geometries and numeration of atoms in *o*-BQ, *p*-BQ, *p*-HQ, and PC are shown in Fig. 1. All atoms of the benzene ring with O atoms in *o*-BQ, *p*-BQ, *p*-HQ, and PC are completely planar. The calculated frequencies of *o*-BQ, *p*-BQ, *p*-HQ, and PC with HF and DFT methods have no imaginary vibrational frequency, indicating that the optimized geometries are reasonable and reliable.

The bond lengths and bond angles of *o*-BQ, PC, *p*-HQ, and *p*-BQ optimized at B3LYP/6-31G (d), B3LYP/6-31G (d, p), HF/6-31G (d), and HF/6-31G (d, p) levels are summarized in Tables 1 and 2, respectively.

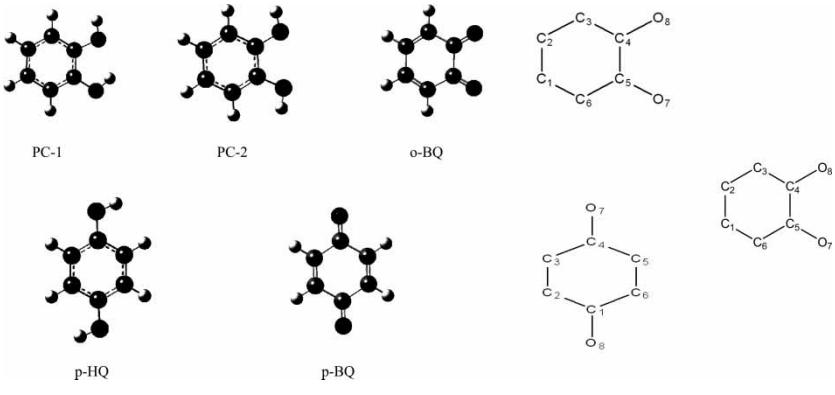

Figure 1. Optimized geometries and numbering in *o*-BQ, *p*-BQ, *p*-HQ, and PC.

Table 1. The geometry parameter of *o*-BQ and PC

	Compound											
	PC-1				PC-2				*o*-BQ			
	Method											
	B3LYP		HF		B3LYP		HF		B3LYP		HF	
	Basis set											
	6-31G (d)	6-31G (d, p)	6-31G (d)	6-31G (d, p)	6-3G (d)	6-3G (d, p)	6-3G (d)	6-3G (d, p)	6-3G (d)	6-3G (d, p)	6-3G (d)	6-3G (d, p)
Bond angle (Å)												
R(1,2)	1.394	1.394	1.381	1.381	1.410	1.391	1.377	1.377	1.463	1.463	1.475	1.475
R(1,6)	1.398	1.398	1.389	1.388	1.399	1.399	1.392	1.391	1.350	1.350	1.328	1.327
R(2,3)	1.399	1.399	1.390	1.389	1.399	1.399	1.392	1.391	1.350	1.350	1.328	1.327
R(3,4)	1.390	1.390	1.378	1.378	1.394	1.394	1.379	1.397	1.474	1.474	1.480	1.480

R(4,5)	1.406	1.406	1.393	1.393	1.410	1.410	1.398	1.398	1.561	1.561	1.546	1.546
R(4,8)	1.380	1.379	1.363	1.362	1.367	1.366	1.352	1.350	1.218	1.218	1.188	1.188
R(5,6)	1.392	1.392	1.379	1.379	1.394	1.394	1.379	1.379	1.474	1.474	1.480	1.480
R(5,7)	1.365	1.364	1.350	1.348	1.367	1.366	1.352	1.350	1.218	1.218	1.188	1.188
Bond angle (°)												
A(1,2,3)	119.8	119.8	119.7	119.7	119.7	119.7	119.6	119.6	122.3	122.3	122.4	122.4
A(2,3,4)	119.8	119.8	120.0	120.0	120.9	120.9	120.9	120.9	120.5	120.5	120.5	120.5
A(3,4,5)	120.5	120.5	120.4	120.4	119.4	119.4	119.4	119.4	117.2	117.2	117.1	117.1
A(3,4,8)	124.6	124.6	124.0	124.0	123.5	123.6	123.2	123.2	122.9	122.9	122.9	122.9
A(5,4,8)	114.8	114.8	115.6	115.6	117.1	117.1	117.4	117.4	119.9	119.9	120.0	120.0
A(4,5,6)	119.5	119.4	119.5	119.5	119.4	119.4	119.4	119.4	117.2	117.2	117.1	117.1
A(4,5,7)	120.3	120.4	120.7	120.7	117.1	117.1	117.4	117.4	119.9	119.9	120.0	120.0
A(6,5,7)	120.2	120.2	119.8	119.8	123.5	123.6	123.2	123.2	122.9	122.9	122.9	122.9
A(1,6,5)	120.1	120.1	120.2	120.2	120.9	120.9	120.9	120.9	120.5	120.5	120.5	120.5
A(2,1,6)	120.2	120.3	120.2	120.2	119.7	119.7	119.6	119.6	122.3	122.3	122.4	122.4

Table 2. The geometry parameter of *p*-HQ and *p*-BQ

	Compound														
	p-HQ					*p*-BQ									
	Method														
	B3LYP		HF		Exp.1[24]	B3LYP		BP86[26]	BLYP[26]	B3P86[26]	B3PW91[26]	HF			Exp. 2[25]
	Basis set														
	6-31G (d)	6-31G (d, p)	6-31G (d)	6-31G (d, p)		6-31G (d)	6-31G (d, p)			6-31G (d, p)		6-31G (d)	6-31G (d, p)	6-31 + G (d, p)[27]	
Bond length (Å)															
R(1,2)	1.399	1.397	1.386	1.386	1.398	1.487	1.486	1.490	1.494	1.481	1.483	1.489	1.489	1.490	1.481
R(1,6)	1.397	1.399	1.384	1.384	1.392	1.487	1.486	1.490	1.494	1.481	1.483	1.489	1.489	1.490	1.481
R(1,8)	1.372	1.372	1.358	1.357	1.377	1.225	1.225	1.223	1.241	1.222	1.223	1.194	1.194	1.195	1.225
R(2,3)	1.394	1.394	1.384	1.384	1.390	1.343	1.343	1.341	1.356	1.341	1.341	1.323	1.323	1.325	1.344
R(3,4)	1.397	1.399	1.384	1.384	1.398	1.487	1.486	1.341	1.356	1.341	1.341	1.489	1.489	1.490	1.481

R(4,5)	1.399	1.397	1.386	1.386	1.392	1.487	1.486	1.490	1.494	1.481	1.483	1.489	1.489	1.490	1.481
R(4,7)	1.372	1.372	1.358	1.357	1.377	1.225	1.225	1.223	1.241	1.222	1.223	1.194	1.194	1.195	1.225
R(5,6)	1.394	1.394	1.384	1.384	1.396	1.343	1.343	1.341	1.356	1.341	1.341	1.323	1.323	1.325	1.334
Bond angle (°)															
A(2,1,6)	119.5	119.5	119.4	119.4	120.0	117.3	117.3	117.3	117.2	117.4	117.3	117.2	117.2		118.1
A(2,1,8)	122.9	122.9	122.8	122.8	123.0	121.4	121.4	121.3	121.4	121.3	121.3	121.4	121.4		121.0
A(6,1,8)	117.6	117.6	117.8	117.8		121.4	121.4	121.3	121.4	121.3	121.3	121.4	121.4		
A(1,2,3)	120.4	120.1	120.5	120.5	120.0	121.4	121.4	121.3	121.4	121.3	121.3	121.4	121.4		121.0
A(2,3,4)	120.1	120.4	120.2	119.4	120.0	121.4	121.4	121.3	121.4	121.3	121.3	121.4	121.4		121.0
A(3,4,5)	119.5	119.5	119.4	120.2	120.0	117.3	117.3	117.3	117.2	117.4	117.3	117.2	117.2		118.1
A(3,4,7)	117.6	117.6	117.8	117.8		121.4	121.4	121.3	121.4	121.4	121.3	121.4	121.4		121.0
A(5,4,7)	122.9	122.9	122.8	122.8	123.0	121.4	121.4	121.3	121.4	121.4	121.3	121.4	121.4		
A(4,5,6)	120.4	120.1	120.5	120.5	120.0	121.4	121.4	121.3	121.4	121.4	121.3	121.4	121.4		121.0
A(1,6,5)	120.1	120.4	120.2	120.2	120.0	121.4	121.4	121.3	121.4	121.4	121.3	121.4	121.4		

Exp, experimental values.

Tables 1 and 2 show that the bond lengths and bond angles of the same molecule optimized using the B3LYP method are in good agreement with those optimized using the HF method, and the geometries of *p*-HQ and *p*-BQ optimized using DFT and HF methods are also consistent with the experimental values[24,25] and calculated results in the literatures.[26,27]

Vibration

The experimental spectra of PC are shown in Fig. 2. The ordinate is the IR relative intensity, and the abscissa represents frequency (cm^{-1}). The calculated vibrational spectrum showed that there were systematic errors between predicted bonds and the experimental spectrum. Scaling of the force constants according to the methods reported by Yamauchi et al.[28] and Pulay et al.[29] is a very useful way to account for systematic error such as the neglect of harmonic effects, basis set defects, and election correlation. In many cases, the typical value for the scaling factors range from 0.7 to 0.99, the scaling factor of B3LYP/6-31G (d), B3LYP/6-31G (d, p), HF/6-31G (d), and HF/6-31G (d, p) is 0.9614, 0.96, 0.8953, and 0.8992[30] to predict the vibrational spectrum of *o*-BQ, *p*-BQ, *p*-HQ, and PC, respectively. The calculated frequencies and experimental frequencies[31] are summarized in Table 3. From Table 3, the results indicate that the calculated spectrum of the same molecule at B3LYP (or HF)/6-31G (d) level are in agreement with that at B3LYP (or HF)/6-31G (d, p) level using the same method.

The good overall agreement with experimental data for PC-1 confirms the reliability of the presented band assignment. It is concluded that the predicted infrared spectrum for the PC-1 investigated here should be reliable. Because there are deviations of the infrared intensities between the experimental data and the calculated spectrum, some peaks could not be found in the experiment but can be found in calculated spectrum. The peaks found not only in the calculated spectrum but also in the experimental spectrum are important, thus we only discuss the peaks found in the experimental spectrum and the peaks of stronger infrared intensities in the calculated spectrum.

The strongest peak in the calculated spectrum of PC-1 appears at 1268 cm^{-1} [B3LYP/6-31G (d)] or 1251 cm^{-1} [HF/6-31G (d)], which represents in-plane bending of CH in benzene ring, whereas the strongest experimental bond is located at 1264 cm^{-1}. Two modes are associated mainly with the OH stretching of PC-1, which are located at 3627 and 3574 cm^{-1} [B3LYP/6-31G (d)] or at 3694 cm^{-1} and 3674 cm^{-1} [HF/6-31G (d)] in the calculated spectrum, and its experimental frequency appears at 3675 cm^{-1} and 3624 cm^{-1}. The CH stretching, CO stretching, and CC stretching of PC-1 in the calculated spectrum are located at 3085 cm^{-1}, 1608 cm^{-1}, and 1504 cm^{-1} [B3LYP/6-31G (d)] or at 3031 cm^{-1}, 1629 cm^{-1}, and 1518 cm^{-1} [HF/6-31G (d)], whereas its experimental frequency appeared at 3086 cm^{-1}, 1616 cm^{-1}, and 1516 cm^{-1}, respectively. Seven modes that

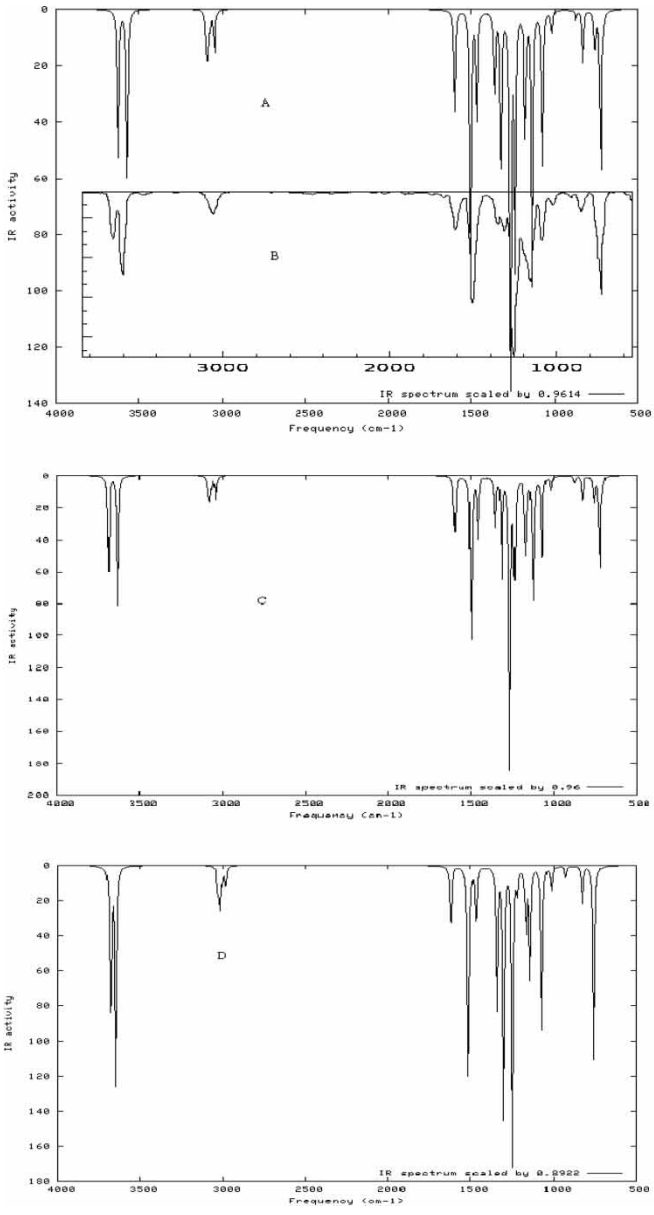

Figure 2. The IR spectra and the predicted spectra of PC-1 and PC-2. A, C, D, and E represent the spectra predicted theoretically for PC-1 at B3LYP/6-31G (d), B3LYP/6-31G (d, p), HF/6-31G (d), and HF/6-31G (d, p) levels, respectively; B represents experimental spectra of PC in gas state[31]; F, G, H, and I represent the spectra predicted theoretically for PC-2 at B3LYP/6-31G (d), B3LYP/6-31G (d, p), HF/6-31G (d), and HF/6-31G (d, p) levels, respectively. The plot of predicted spectra was drawn with the GaussSum 0.8 package.

(*continued*)

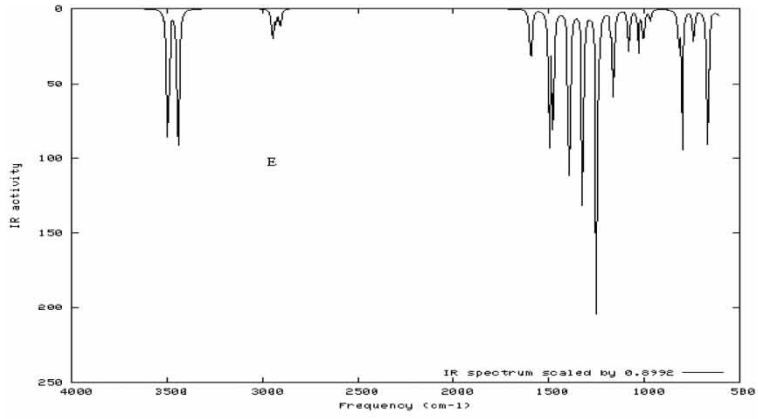

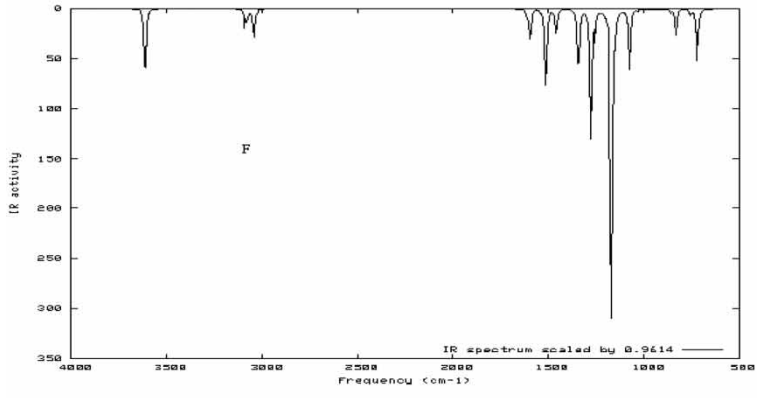

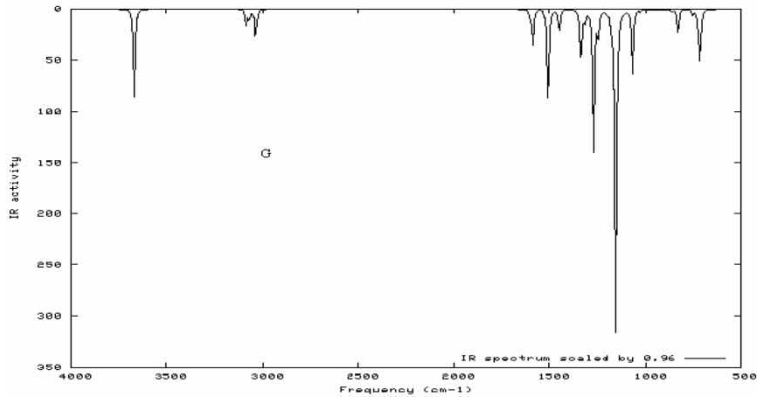

Figure 2. Continued.

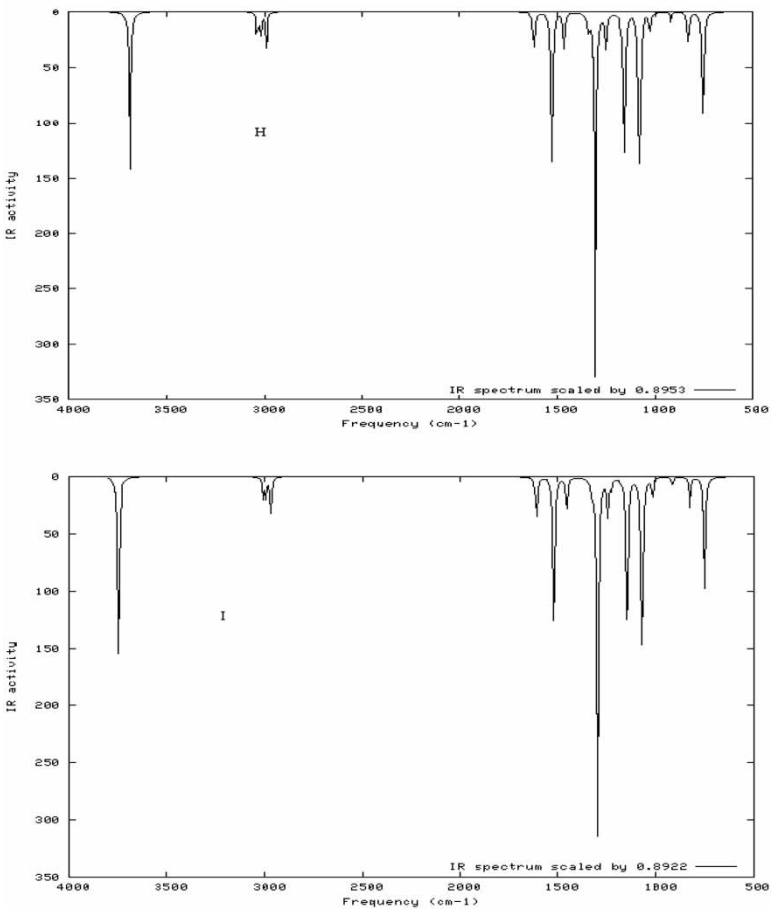

Figure 2. Continued.

predicted in-plane bending of CH or OH in the ring of PC-1 were located at 1364 cm^{-1}, 1326 cm^{-1}, 1268 cm^{-1}, 1177 cm^{-1}, 1137 cm^{-1}, 1075 cm^{-1}, and 757 cm^{-1} [B3LYP/6-31G (d)] or at 1347 cm^{-1}, 1306 cm^{-1}, 1251 cm^{-1}, 1168 cm^{-1}, 1077 cm^{-1}, 1072 cm^{-1}, and 755 cm^{-1} [HF/6-31G (d)] and are allowed in the IR spectrum at 1368 cm^{-1}, 1328 cm^{-1}, 1264 cm^{-1}, 1176 cm^{-1}, 1103 cm^{-1}, 1037 cm^{-1}, and 748 cm^{-1}, respectively. Two modes of out-plane bending located at 917 cm^{-1} and 757 cm^{-1} [B3LYP/6-31G (d)] or at 977 cm^{-1} and 933 cm^{-1} [HF/6-31G (d)] were assigned to bands at 865 cm^{-1} and 748 cm^{-1}, respectively.

Compared with PC-1, except for OH stretching of PC-2, the frequencies of other modes change slightly, and only one frequency of OH stretching of PC-2 is found in the theoretical spectrum, which is different from that in the experimental IR. Therefore, PC-1 is more stable than PC-2.

Table 3. The calculated frequencies (cm^{-1}) of PC-1, PC-2, and *o*-BQ

	B3LYP $\upsilon_{Cal}(cm^{-1})$(Km/mol)				HF $\upsilon_{Cal}(cm^{-1})$(Km/mol)			
	6-31G (d)		6-31G (d, p)		6-31G (d)		6-31G (d, p)	
Exp.[31]		Scaled by 0.9614		Scaled by 0.96		Scaled by 0.8953		Scaled by 0.8992
PC-1								
	188 (15)	181	188 (19)	180	174 (185)	156	172 (178)	155
	227 (163)	218	221 (150)	212	210 (1)	188	210 (1)	189
	300 (3)	288	300 (3)	288	329 (0)	296	329 (0)	296
	311 (7)	299	311 (5)	299	339 (5)	304	339 (5)	305
	427 (66)	411	426 (66)	409	395 (118)	354	397 (118)	357
	447 (7)	430	448 (7)	430	483 (8)	432	484 (8)	435
	462 (5)	444	461 (5)	443	508 (1)	455	508 (0)	457
	560 (9)	538	560 (9)	538	600 (11)	537	601 (11)	540
	568 (0)	546	568 (0)	545	620 (0)	555	620 (0)	558
	590 (0)	567	590 (2)	566	635 (2)	569	632 (2)	568
	698 (0)	671	698 (0)	670	782 (0)	700	782 (0)	703
	752 (61)	723	752 (58)	722	784 (0)	702	784 (87)	705
748	787 (19)	757	787 (19)	756	843 (90)	755	843 (22)	758
	840 (0)	808	840 (0)	806	923 (21)	826	924 (20)	743
	862 (19)	829	862 (19)	828	956 (0)	856	953 (0)	857
865	908 (4)	873	912 (4)	876	1042 (8)	933	1043 (8)	938
931	954 (0)	917	958 (0)	920	1091 (0)	977	1091 (0)	981
	1059 (9)	1018	1057 (9)	1015	1133 (16)	1014	1134 (16)	1020
1037	1118 (62)	1075	1115 (66)	1070	1198 (102)	1072	1194 (102)	1074

1103	1183 (97)	1137	1174 (93)	1127	1203 (0)	1077	1200 (2)	1079
	1187 (0)	1141	1182 (0)	1135	1279 (72)	1145	1272 (72)	1144
1176	1224 (44)	1177	1216 (53)	1167	1305 (38)	1168	1300 (95)	1169
	1290 (87)	1240	1288 (83)	1236	1362 (14)	1219	1356 (17)	1219
1264	1319 (175)	1268	1317 (183)	1264	1397 (174)	1251	1396 (165)	1255
1328	1379 (71)	1326	1370 (64)	1315	1459 (165)	1306	1455 (171)	1308
1368	1419 (36)	1364	1413 (30)	1356	1505 (82)	1347	1494 (74)	1343
	1524 (42)	1465	1518 (38)	1457	1644 (38)	1472	1639 (35)	1474
1516	1564 (107)	1504	1560 (115)	1500	1695 (155)	1518	1692 (169)	1521
	1669 (28)	1604	1666 (31)	1599	1814 (29)	1624	1812 (32)	1629
1616	1673 (14)	1608	1669 (11)	1602	1819 (16)	1629	1817 (14)	1634
	3168 (15)	3046	3166 (14)	3039	3344 (16)	2994	3228 (14)	2903
	3194 (6)	3071	3191 (6)	3063	3368 (9)	3015	3351 (8)	3013
3086	3209 (20)	3085	3206 (17)	3078	3386 (24)	3031	3368 (22)	3029
	3219 (10)	3095	3216 (8)	3087	3397 (12)	3041	3379 (11)	3038
3622	3718 (77)	3574	3784 (79)	3632	4092 (132)	3664	4168 (131)	3748
3675	3773 (57)	3627	3844 (61)	3690	4126 (104)	3694	4204 (107)	3780
PC-2								
	182 (0)	175	182 (0)	175	200 (0)	179	199 (0)	179
	291 (34)	280	290 (37)	278	274 (0)	245	266 (0)	239
	312 (12)	300	313 (12)	300	279 (241)	250	272 (245)	245
	337 (0)	324	334 (0)	321	338 (13)	303	340 (13)	306
	355 (211)	341	353 (200)	339	342 (52)	306	341 (43)	307
	454 (4)	436	455 (4)	437	491 (5)	440	492 (5)	442
	465 (0)	447	464 (0)	445	510 (1)	457	510 (10	459
	546 (5)	525	547 (5)	525	587 (7)	526	588 (6)	529

(*continued*)

Table 3. Continued

	B3LYP $\upsilon_{Cal}(cm^{-1})$(Km/mol)				HF $\upsilon_{Cal}(cm^{-1})$(Km/mol)			
	6-31G (d)		6-31G (d, p)		6-31G (d)		6-31G (d, p)	
Exp.[31]		Scaled by 0.9614		Scaled by 0.96		Scaled by 0.8953		Scaled by 0.8992
	572 (0)	550	572 (0)	549	624 (0)	559	624 (0)	561
	595 (0)	572	595 (0)	571	640 (1)	573	640 (1)	575
	705 (0)	678	704 (0)	676	785 (0)	703	785 (0)	706
	745 (66)	716	747 (63)	717	838 (7)	750	837 (92)	753
748	783 (6)	753	782 (6)	751	839 (99)	751	838 (6)	754
	828 (0)	796	827 (0)	794	925 (28)	828	925 (29)	832
	863 (26)	830	862 (26)	828	944 (0)	845	941 (0)	846
865	890 (4)	856	895 (3)	859	1027 (8)	919	1028 (8)	924
931	943 (0)	907	948 (0)	910	1084 (0)	971	1084 (0)	975
	1072 (2)	1031	1070 (2)	1027	1144 (17)	1024	1141 (18)	1026
1037	1116 (61)	1073	1112 (62)	1068	1199 (56)	1073	1196 (56)	1075
1103	1190 (0)	1144	1184 (0)	1137	1208 (129)	1082	1204 (133)	1083
	1198 (14)	1152	1190 (13)	1142	1291 (22)	1156	1286 (20)	1156
1176	1215 (210)	1168	1204 (315)	1156	1294 (124)	1159	1286 (138)	1156
	1303 (28)	1253	1300 (29)	1248	1384 (8)	1239	1376 (8)	1237
1264	1328 (136)	1277	1325 (139)	1272	1398 (30)	1252	1396 (32)	1255
1328	1384 (14)	1331	1373 (13)	1318	1457 (335)	1304	1453 (315)	1307
1368	1399 (70)	1345	1359 (59)	1305	1497 (15)	1340	1486 (14)	1336
	1513 (28)	1455	1507 (27)	1447	1635 (32)	1464	1629 (32)	1465
1516	1573 (96)	1512	1569 (103)	1506	1707 (136)	1528	1702 (148)	1530

	1660 (34)	1596	1658 (35)	1591	1808 (33)	1619	1806 (33)	1624
1616	1678 (7)	1613	1674 (9)	1607	1822 (7)	1631	1818 (8)	1635
	3163 (29)	3041	3162 (26)	3036	3341 (30)	2991	3325 (27)	2990
	3166 (7)	3044	3164 (7)	3037	3343 (7)	2993	3328 (7)	2993
3086	3197 (13)	3074	3195 (12)	3067	3372 (19)	3019	3356 (18)	3018
	3214 (18)	3090	3211 (16)	3082	3391 (22)	3036	3374 (20)	3034
3622	3756 (70)	3611	3824 (76)	3671	4120 (150)	3689	4199 (155)	3776
3675	3757 (10)	3612	3825 (10)	3672	4121 (13)	3689	4200 (14)	3777
o-BQ								
	84 (0)	80	84 (0)	81	77 (0)	69	78 (0)	70
	229 (4)	220	229 (4)	220	250 (8)	224	250 (8)	245
	348 (4)	336	348 (4)	334	385 (6)	345	384 (6)	345
	420 (0)	404	420 (0)	403	450 (0)	403	450 (0)	405
	438 (3)	421	438 (3)	420	468 (4)	419	468 (4)	421
	473 (0)	455	473 (0)	454	519 (1)	465	520 (1)	468
	550 (0)	529	550 (0)	528	593 (0)	531	593 (0)	533
	556 (16)	535	556 (15)	534	599 (23)	536	599 (23)	539
	677 (2)	651	676 (2)	649	740 (3)	663	739 (3)	665
	743 (74)	714	742 (72)	712	826 (111)	740	825 (109)	742
	788 (0)	758	788 (0)	756	863 (0)	772	863 (0)	776
	882 (0)	848	881 (0)	846	949 (0)	850	948 (0)	852
748	896 (0)	861	896 (0)	760	982 (0)	879	981 (0)	882
	969 (1)	932	967 (1)	928	1015 (1)	909	1013 (1)	911
	1005 (0)	966	1007 (0)	967	1132 (1)	1013	1131 (1)	1017
865	1027 (0)	987	1027 (0)	986	1146 (0)	1026	1143 (0)	1028
931	1333 (13)	1089	1131 (13)	1085	1126 (26)	1008	1224 (26)	1101

(*continued*)

Table 3. Continued

	B3LYP $\upsilon_{Cal}(cm^{-1})$(Km/mol)				HF $\upsilon_{Cal}(cm^{-1})$(Km/mol)			
	6-31G (d)		6-31G (d, p)		6-31G (d)		6-31G (d, p)	
Exp.[31]		Scaled by 0.9614		Scaled by 0.96		Scaled by 0.8953		Scaled by 0.8992
	1164 (20)	1119	1160 (18)	1114	1260 (17)	1128	1255 (15)	1128
1037	1194 (2)	1148	1186 (1)	1139	1290 (1)	1155	1283 (1)	1154
1103	1282 (48)	1232	1277 (48)	1226	1409 (79)	1261	1405 (78)	1263
	1402 (0)	1348	1395 (0)	1339	1516 (0)	1357	1510 (0)	1358
1176	1449 (27)	1394	1442 (49)	1384	1565 (40)	1401	1559 (43)	1402
	1626 (3)	1563	1625 (3)	1560	1812 (1)	1622	1812 (1)	1629
1264	1696 (1)	1631	1693 (1)	1625	1861 (0)	1666	1860 (0)	1673
1328	1758 (190)	1690	1758 (190)	1688	2022 (295)	1810	2023 (295)	1819
1368	1787 (50)	1718	1787 (49)	1716	2028 (101)	1816	2028 (100)	1824
	3187 (6)	3064	3183 (6)	3056	3371 (6)	3018	3351 (7)	3013
1516	3199 (11)	3076	3194 (10)	3066	3383 (11)	3029	3363 (9)	3024
	3218 (9)	3094	3213 (8)	3084	3404 (6)	3047	3384 (5)	3043
1616	3221 (4)	3097	3216 (4)	3087	3406 (4)	3049	3387 (4)	3046

Most bands of o-BQ observed at B3LYP/6-31G (d) or 6-31G (d, p) levels are in good agreement with those at HF/6-31G (d) or 6-31G (d, p) levels, indicating that the geometries of *o*-BQ are reliable.

Electrochemical Behavior of PC

The electrochemistry of PC has been studied widely.[32,33] The peak potentials are associated with the pH in the solution, they shift negatively with increasing pH according to the relations of oxidation peak potential (E^{ox}) (V) = 1.052–0.0610 pH. This is in accordance with a $2H^+/2e^-$ stoichiometry for the oxidation process of PC; the oxidation of PC to *o*-BQ follows the simple stoichiometry PC = *o*-BQ + $2H^+ + 2e^-$.

The cyclic voltammagram at a gold electrode for the oxidation of 1 mM PC in 0.1 M phosphate buffer at pH 7.3 is shown in Fig. 3. The cyclic voltammagram exhibits a chemically reversible oxidation process, as indicated by similar sized peaks for the forward and reverse scan, with an oxidation peak potential (E^{ox}) of 0.190 V and reduction peak potential (E^{red}) of 0.090 V versus SCE; the rate of current (i_{ox}/i_{red}) is 1.01. Because of the conditional potential $E^{of} = (E^{ox} + E^{red})/2$,[34] E^{of} was calculated as below:

$$\text{pH} = 7.30, \quad E^{of} = (0.190\,\text{V} + 0.090\,\text{V})/2 = 0.140\,\text{V},$$

so, the standard potential (E_1^0) versus SCE is written as

$$E^{of} = E_1^0 + 0.059 \log [H^+]\ (298.15\,\text{K}),$$

then,

$$\text{pH } 7.30, \quad E_1^0 = 0.571\,\text{V}\ (298.15\,\text{K}).$$

The standard potential (E^o) versus normal hydrogen electrode (NHE) is given as

$$E^o = E_1^0 + E_{SCE}^0,$$

where E_{SCE}^0[35] represents the standard electrode potential for Hg_2Cl_2/Hg, therefore, E^o is calculated as below

$$\text{pH} = 7.30, \quad E^o = 0.571\,\text{V} + 0.2416\,\text{V} = 0.813\,\text{V}\ (1\,\text{atm}, 298.15\,\text{K}).$$

Theoretical Calculation of Standard Electrode Potential (E^0) of Half Reaction for *o*-BQ and PC

The redox reaction in solution is as shown in Fig. 4. PC_g, *o*-BQ_g, *p*-BQ_g, and *p*-HQ_g represent PC, *o*-BQ, *p*-BQ, and *p*-HQ in the gas state, respectively.

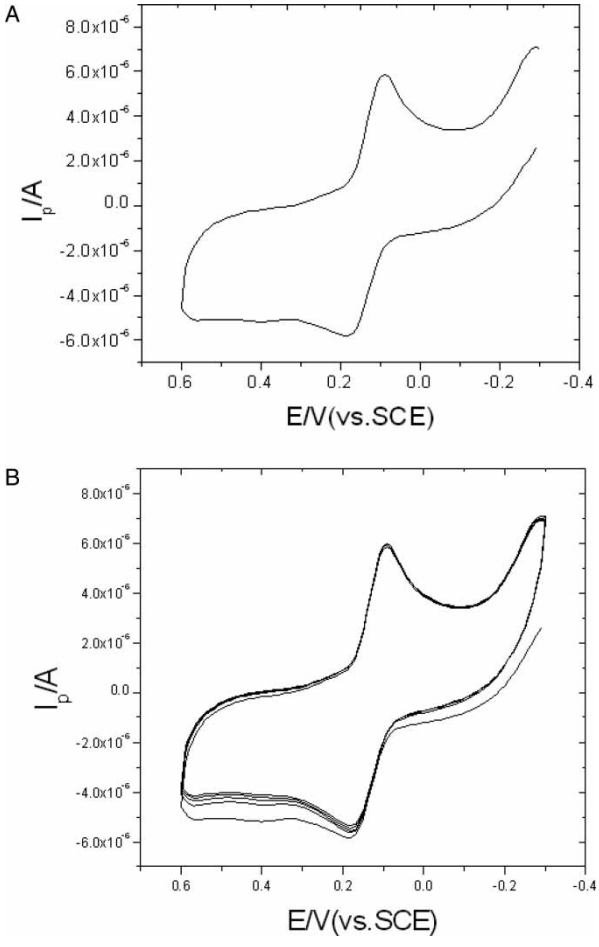

Figure 3. Cyclic voltammagram for the oxidation of 1.0 mM PC in 0.1 M phosphate at pH 7.30. The cyclic voltammagrams were obtained in a stationary solution with a 1-mm-radius gold disk as a working electrode and using a potential scan rate of 0.1 V s^{-1} (A), One scan; (B), three scans.

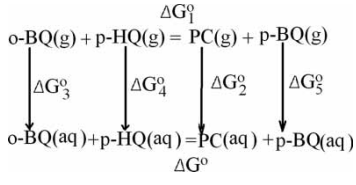

Figure 4. The scheme of redox reaction for PC and *o*-BQ in solution; g and aq denote gas and solution, respectively.

Table 4. The calculated thermochemistry values, the ΔrG^0 (1 atm, 298.15 K), and the standard electrode potential (E^0)

	Compound															
	PC-1				*o*-BQ				*p*-HQ				*p*-BQ			
	Method															
	B3LYP		HF		B3LYP		HF		B3LYP		HF		B3LYP		HF	
	Basis set															
	6-31G (d)	6-31G (d, p)	6-31G (d)	6-31G (d, p)	6-31G (d)	6-31G (d, p)	6-31G (d)	6-31G (d, p)	6-31G (d)	6-31G (d, p)	6-31G (d)	6-31G (d, p)	6-31G (d)	6-31G (d, p)	6-31G (d)	6-31G (d, p)
G^0 (Hartree)	−382.6 03311	−382.6 20842	−380.3 26477	−380.3 47045	−381.3 85932	−381.3 92250	−379.15 9450	−379.1 66795	−382.5 99389	−382.6 17607	−380.3 23395	−380.3 44026	−381.3 95530	−381.4 03087	−379.1 72139	−379.1 80756
ΔrG_1^0 (KJ mol^{-1})	−35.50	−36.95	−41.41	−42.60												
ΔrG_2^0 (KJ mol^{-1})	−35.36	−35.15	−38.87	−42.93												
ΔrG_3^0 (KJ mol^{-1})					−28.97	−29.30	−46.19	−40.92								
ΔrG_4^0 (KJ mol^{-1})									−48.99	−48.74	−53.80	−53.75				
ΔrG_5^0 (KJ mol^{-1})													−16.05	−16.64	−25.16	−26.04
ΔrG_6^0 (KJ mol^{-1})	26.55	26.25	35.96	25.70												
ΔrG^0 (KJ mol^{-1})	−8.95	−10.70	−5.45	−16.90												
E^0	0.745	0.754	0.727	0.787												
K	9.28×10^{10}	1.21×10^{11}	4.56×10^{10}	3.69×10^{11}												

The transformed Gibbs free energy in the gas state is written as

$$\Delta rG^{o}_{1}(298.15\,\mathrm{K}) = G^{o}_{\mathrm{PCg}} + G^{o}_{o\text{-BQg}} - G^{o}_{o\text{-BQg}} - G^{o}_{p\text{-HQg}},$$

where G^{o} represents the standard Gibbs free energies at 298.15 K, 1 atm, which is calculated through the Gaussian 03 package.

ΔrG^{o}_{2}, ΔrG^{o}_{3}, ΔrG^{o}_{4}, and ΔrG^{o}_{5} are the solvation energies for PC, *o*-BQ, *p*-HQ, and *p*-BQ in water at 298.15 K, 1 atm, respectively.

If

$$\Delta rG^{o}_{6} = \Delta rG^{o}_{2} + \Delta rG^{o}_{5} - \Delta rG^{o}_{3} - \Delta rG^{o}_{4},$$

then the standard transformed Gibbs energy of reaction in solution is written as

$$\Delta rG^{o}(298.15\,\mathrm{K}, 1\,\mathrm{atm}) = \Delta rG^{o}_{1} + \Delta rG^{o}_{6}$$

Standard electrode potential (E^{0}) of half reaction for *o*-BQ, H^{+}/PC is calculated as

$$\Delta rG^{o}(298.15\,\mathrm{K}, 1\,\mathrm{atm}) = -nF(E^{o} - E^{0}_{p\text{-BQ.H}^{-}/p\text{-HQ}})$$

$$\Delta rG^{o}(298.15\,\mathrm{K}, 1\,\mathrm{atm}) = -RT\ln K$$

where K represents the equilibrium constant at 298.15 K, 1 atm, $E^{o}_{p\text{-BQ}/p\text{-HQ}}$ is 0.699 V.[35] The thermochemistry values calculated from Gaussian03 for reaction (3) are shown in Table 4, ΔrG(298.15 K, 1 atm) for the reaction (3) and the standard electrode potential (E^{0}) of half reaction for *o*-BQ and PC-1 were also calculated. From Table 4, the standard electrode potential with PC-1 calculated using B3LYP/6-31G (d), B3LYP/6-31G (d, p), HF/6-31G (d), and HF/6-31G (d, p) methods are 0.745 V, 0.754 V, 0.727 V, and 0.787 V, respectively, which are in good agreement with the experimental value of 0.813 V.

CONCLUSIONS

The geometries, vibration of *o*-BQ and PC, and the standard electrode potential for half reaction of *o*-BQ and PC with a *p*-BQ, H^{+}/*p*-BQ reference electrode were calculated using B3LYP/6-31G (d), B3LYP/6-31G (d, p), HF/6-31G (d), and HF/6-31G (d, p) methods, respectively. Two conformers of PC are computed; the oxidized PC at the electrode can be identified by comparison of theoretical vibration with experimental spectra. The predicted standard potential of half reaction for *o*-BQ and PC using DFT and HF methods were in agreement with the experimental result.

ACKNOWLEDGMENTS

This research was supported by the National Sciences Foundation of China (no. 20302002) and the Foundation of Jiangsu Province Key Laboratory for Chemistry of Low-Dimensional Materials (no. JSKC06031).

REFERENCES

1. Kim, S. H.; Lee, J. W.; Ye, I. Spectroelectrochemical and electrochemical behavior of epinephrine at a gold electrode. *Electrochem. Acta* **2000**, *45*, 2889–2895.
2. Fike, R. R.; Curran, D. J. Determination of catecholamines by thin-layer linear sweep voltammetry. *Anal. Chem.* **1977**, *49*, 1205–1210.
3. Hawley, M. D.; Tatawawadi, S. V.; Piekarski, S.; Adams, R. N. Electrochemical studies of the oxidation pathways of catecholamines. *J. Am. Chem. Soc.* **1967**, *89*, 447–450.
4. Song, Y. Z.; Zhou, J. F.; Song, Y.; Wei, Y. G.; Wang, H. Density-functional theory studies on standard electrode potentials of half reaction for L-adrenaline and adrenalinequinone. *Bioor. Med. Chem. Lett.* **2005**, *15*, 4671–4680.
5. Christenson, R. H.; Meglothlin, C. D. Elucidation of metanephrine to normetanephrine and epinephrine to norepinephrine ratios by fluorescence derivative spectroscopy. *Anal. Chem.* **1982**, *54*, 2015–2017.
6. Wu, X.; Mu, L.; Zhang, W. Impedance of the electrochemical oxidation of epinephrine on a glassy carbon electrode. *J. Electroanal. Chem.* **1993**, *352*, 295–300.
7. Sucheta, A.; Rusling, F. J. Effect of background charge on estimating diffusion coefficients by chronocoulometry at glassy carbon electrodes. *Electroanalysis* **1991**, *3*, 735–739.
8. Deakin, M. R.; Kovach, P. M.; Stutle, K. J.; Wightman, R. M. Heterogeneous mechanisms of the oxidation of catechols and ascorbic acid at carbon electrodes. *Anal. Chem.* **1986**, *58*, 1474–1480.
9. Wightman, R. M.; May, L. J.; Michael, A. C. Fast-scan voltammetry of biogenic amines. *Anal. Chem.* **1988**, *60*, 1268–1272.
10. Song, Y. Z.; Song, Y.; Xie, W.; Shi, D. The electrochemical behavior of dopamine at glassy carbon electrode modified by nafion multiwalled carbon nanotubes. *Russian J. Phys. Chem.* **2006**, *80*, 1467–1474.
11. Alberty, R. A. Calculation of standard transformed gibbs energies and standard transformed enthalpies of biochemical reactants. *Arch. Biochem. Biophys.* **1998**, *353*, 116–130.
12. Wagman, D. D.; Evans, W. H.; Parker, V. B.; Schumm, R. H.; Hallow, I.; Bailey, S. M.; Churney, K. L.; Nuttall, R. L. The NBS tables of chemical themodynamic properties. *J. Phys. Chem. Ref. Data* **1982**, *11,* (Suppl. 2), 2–158.
13. Alberty, R. A. Calculation of standard transformed formation properties of biochemical reactants and standard opparent reduction potentials of half reactions. *Biochem. Biophys. Acta* **1998**, *358*, 25–39.
14. Frisch, M. J.; Trucks, G. W.; Schlegel, H. B.; Scuseria, G. E.; Robb, M. A.; Cheeseman, J. R.; Montgomery, J. A., Jr.; Vreven, T.; Kudin, K. N.; Burant, J. C.; Millam, J. M.; Iyengar, S. S.; Tomasi, J.; Barone, V.; Mennucci, B.; Cossi, M.; Scalmani, G.; Rega, N.; Petersson, G. A.; Nakatsuji, H.; Hada, M.; Ehara, M.; Toyota, K.; Fukuda, R.; Hasegawa, J.; Ishida, M.; Nakajima, T.; Honda, Y.; Kitao, O.; Nakai, H.; Klene, M.; Li, X.;

Knox, J. E.; Hratchian, H. P.; Cross, J. B.; Adamo, C.; Jaramillo, J.; Gomperts, R.; Stratmann, R. E.; Yazyev, O.; Austin, A. J.; Cammi, R.; Pomelli, C.; Ochterski, J. W.; Ayala, P. Y.; Morokuma, K.; Voth, G. A.; Salvador, P.; Dannenberg, J. J.; Zakrzewski, V. G.; Dapprich, S.; Daniels, A. D.; Strain, M. C.; Farkas, O.; Malick, D. K.; Rabuck, A. D.; Raghavachari, K.; Foresman, J. B.; Ortiz, J. V.; Cui, Q.; Baboul, A. G.; Clifford, S.; Cioslowski, J.; Stefanov, B. B.; Liu, G.; Liashenko, A.; Piskorz, P.; Komaromi, I.; Martin, R. L.; Fox, D. J.; Keith, T.; Al-Laham, M. A.; Peng, C. Y.; Nanayakkara, A.; Challacombe, M.; Gill, P. M. W.; Johnson, B.; Chen, W.; Wong, M. W.; Gonzalez, C.; Pople, J. A. Gaussian, Inc.: Pittsburgh, PA, 2003.

15. Lee, C.; Yank, W.; Parr, R. G. Development of the Colle-Salvetti correlation-energy formula into a functional of the electron density. *Phys. Rev*. **1988**, *378*, 785–789.
16. Becke, A. D. Density-functional thermochemistry. III. The role of exact exchange. *Chem. Phys.* **1993**, *98* (1), 5648–5652.
17. Foresman, J. B.; Frish, A. E. *Exploring Chemistry with Electronic Structure Methods*; Gaussian, Inc.: Pittsburgh, PA, 1996.
18. Jensen, F. *Introduction to Computational Chemistry*; Wiley: Chichester, 1999.
19. Hariharan, P. A.; Pople, J. A. The influence of polarization functions on molecular orbital hydrogenation energies. *Theor. Chim. Acta* **1973**, *28*, 213–222.
20. Hehre, W. J.; Radom, L.; Schleyer, P. V. R.; Pople, J. A. *Ab Inito Molecular Orbital Theory*; Wiley: New York, 1986.
21. Bonaccorsi, R.; Tomasi, R.; Cimiraglia, Ab initio evaluation of absorption and emission transitions for molecular solutes, including separate consideration of orientational and inductive solvent effects. *J. Comput. Chem.* **1983**, *4*, 567–577.
22. Pascualahuir, J. L.; Silla, E.; Tomasi, J.; Bonaccorsi, R. J. Electrostatic interaction of a solute with a continuum. Improved description of the cavity and of the surface cavity bound charge distribution. *Comput. Chem.* **1987**, *8*, 778–787.
23. Miertus, S.; Scrocco, E.; Tomasi, J. Electrostatic interaction of a solute with a continuum. A direct utilizaion of AB initio molecular potentials for the prevision of solvent effects. *Chem. Phys.* **1981**, *55*, 117–129.
24. Caminati, W.; Melandri, S.; Favero, L. B. Microwave spectroscopy of hydroquinone: The rotational spectrum of the cis conformer. *J. Chem. Phys.* **1994**, *100*, 8569–8572.
25. Hagen, K.; Hedbery, K. J. Reinvestigation of the molecular structure of gaseous *p*-benzoquinone by electron diffraction. *J. Chem. Phys.* **1973**, *59*, 158–162.
26. Uno, B.; Okumura, N.; Goto, M.; Kano, K. n-σ Charge-transfer interaction and molecular and electronic structural properties in the hydrogen-bonding systems consisting of p-quinone dianions and methyl alcohol. *J. Org. Chem.* **2000**, *65*, 1448–1455.
27. Mohandas, P.; Umapathy, S. Density-functional studies on the structure and vibrational spectra of transient intermediates of p-benzoquinone. *J. Phys. Chem. A* **1997**, *101*, 4449–4459.
28. Yamauchi, Y.; Frisch, M.; Gaw, J.; Schaefer, H. F., III. Analytic evaluation and basis set dependence of intensities of infrared spectra. *J. Chem. Phys.* **1986**, *84*, 2262–2278.
29. Pulay, D.; Fogarasi, G.; Pang, F. F.; Boggs, J. E. Systematic ab initio gradient calculation of molecular geometries, force constants, and dipole moment deriva. *J. Am. Chem. Soc.* **1979**, *101*, 2550–2560.

30. Scott, A. P.; Radom, L. Harmonic vibrational frequencies: an evaluation of Hartree-Fock, Møller-Plesset, quadratic configuration interaction, density functional theory, and semiempirical scale factors. *J. Phys. Chem.* **1996**, *100*, 16502–16513.
31. NIST Chemistry WebBook. Available at http://webbook.nist.gov/chemistry.
32. Shahrokhian, S.; Hamzehloei, A. Electrochemical oxidation of catechol in the presence of 2-thiouracil: application to electro-organic synthesis. *Electrochem. Commun.* **2003**, *5*, 706–710.
33. Shahrokhian, S.; Aandanna, A. Mercaptotriazole as a nucleophile in addition to *o*-quinone electrochemically derived from catechol: application to electrosynthesis of a new group of triazole compounds **2005**, *7*, 68–73.
34. Wang, J. *Analytical Electrochemistry*, Second edn.; John Wiley & Sons: New York, 2000.
35. Dobos, D. Electrochemical data. *A Handbook for Electrochemists in Industry and Universities*; Elsevier Scientific Publishing Company: Amsterdam-Oxford, New York, 1975; pp. 88–89.